Substituent Effects of Porphyrin Monolayers on the Structure and Photoelectrochemical Properties of Self-Assembled Monolayers of Porphyrin on Indium−Tin Oxide Electrode

Hiroshi Imahori,*,† Kohei Hosomizu,† Yukie Mori,† Tomoo Sato,‡ Tae Kyu Ahn,§,|| Seong Keun Kim,|| Dongho Kim,*,§ Yoshinobu Nishimura,⊥,# Iwao Yamazaki,*,⊥ Hirotake Ishii,† Hiroki Hotta,† and Yoshihiro Matano†

Department of Molecular Engineering, Graduate School of Engineering, Kyoto University, PRESTO, Japan Science and Technology Agency (JST), Katsura, Nishikyo-ku, Kyoto 615-8510, Japan, Fukui Institute for Fundamental Chemistry, Kyoto University, 34-4, Takano-Nishihiraki-cho, Sakyo-ku, Kyoto 606-8103, Japan, Department of Chemistry, University of Tsukuba, Tsukuba, Ibaraki 305-8571, Japan, Center for Ultrafast Optical Characteristics Control, Department of Chemistry, Yonsei University, Seoul 120-749, Korea, School of Chemistry, Seoul National University, Seoul 151-747, Korea, and Department of Molecular Chemistry, Graduate School of Engineering, Hokkaido University, Sapporo 060-8628, Japan

Received: November 27, 2003; In Final Form: January 22, 2004

Self-assembled monolayers (SAMs) of porphyrins have been prepared to examine the substituent effects of porphyrin monolayers on the structure and photoelectrochemical properties of the SAMs on an ITO electrode. The ultraviolet (UV)−visible absorption, steady-state fluorescence, and cyclic voltammetry measurements for the porphyrin SAMs revealed that the interaction between the porphyrins without bulky *tert*-butyl groups is much larger than that of the porphyrins with bulky *tert*-butyl groups. Photoelectrochemical measurements were performed in nitrogen-saturated Na_2SO_4 aqueous solution containing triethanolamine as an electron sacrificer using the modified ITO working electrode, a platinum wire counter electrode, and an Ag/AgCl reference electrode. The internal quantum yields of photocurrent generation together with the porphyrin fluorescence lifetimes remain virtually the same irrespective of the steric hindrance, which is in sharp contrast with severe self-quenching of the porphyrin excited singlet state in conventional molecular assemblies such as Langmuir−Blodgett films. The two-dimensional, densely packed structure of the porphyrins in SAM is responsible for the long-lived excited singlet state, which is similar to the antenna function of photosystem I in cyanobacteria. These results will provide valuable information on the construction of artificial light-harvesting systems.

Introduction

Energy transfer (EN) and electron transfer (ET) in organized molecular assemblies constitute a topic of great interest owing to the vital roles in biological processes.[1] In particular, photoinduced EN in organized media have merited special attention relevant to antenna function in light-harvesting systems.[2] Namely, the antenna complex is responsible for the collection of light and the subsequent EN to a special pair of chlorophylls in the reaction center, where a charge separation (CS) across the membrane takes place. The resulting charge-separated state is eventually converted into chemical energy. Light-harvesting systems show a great variety in their structures. For instance, in purple bacteria, chlorophylls are organized in symmetric ring-like structures,[3] whereas in green bacteria chlorophylls are arranged into rodlike aggregates.[4] In contrast, chlorophyll aggregates in photosystem (PS) I of cyanobacteria exhibit a rather random array forming two-dimensional structures surrounding the reaction center.[5] Such diversity in natural light-harvesting systems has made it difficult to understand the unique relationship between structure and function in the light-harvesting systems, thereby precluding the successful development of the artificial light-harvesting systems.[6]

In this context, self-assembled monolayers (SAMs) have been attractive candidates for artificial photosynthetic systems because they are relatively stable and can be readily formed in a highly ordered manner on conducting or semiconducting substrates.[7] More importantly, SAMs of photoactive molecules on the substrates can have two-dimensional, densely packed structures, which are in sharp contrast with conventional covalently linked chromophore arrays[8,9] and molecular assemblies in LB films and lipid bilayers.[10−13] SAMs of porphyrins and related compounds on gold and ITO surfaces have thereby attracted considerable attention as artificial light-harvesting and CS systems.[14−19] We have prepared a variety of photoactive SAMs comprising porphyrin, which reveal photoinduced multistep ET and energy transfer (EN) on gold[16−18] or ITO[19] surfaces. In these systems, the structure and photoelectrochemical properties of porphyrins in SAMs may be affected by other surrounding porphyrins in SAMs. However, the substituent effects of porphyrins in SAMs have not been fully addressed.

We report herein the substituent effects of the porphyrin moieties on the structure and photoelectrochemical properties of porphyrin SAMs on ITO electrode (Figure 1) in detail based on the UV−visible absorption, steady-state fluorescence, cyclic

* To whom correspondence should be addressed. E-mail: (H.Imahori) imahori@scl.kyoto-u.ac.jp; (D.K.) dongho@yonsei.ac.kr; (I.Y.) yamiw@eng.hokudai.ac.jp.
† Kyoto University.
‡ University of Tsukuba.
§ Yonsei University.
|| Seoul National University.
⊥ Hokkaido University.
Present address: University of Tsukuba.

10.1021/jp037625e CCC: $27.50
Published on Web 03/30/2004

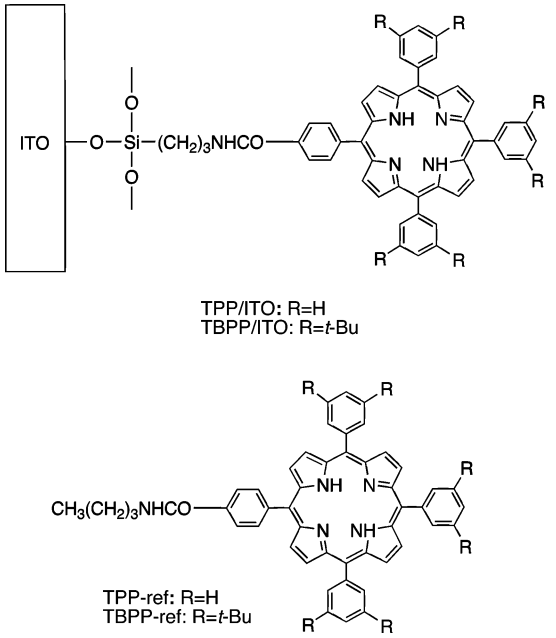

Figure 1. Self-assembled monolayers of porphyrins with different substituents on ITO electrode and the porphyrin references.

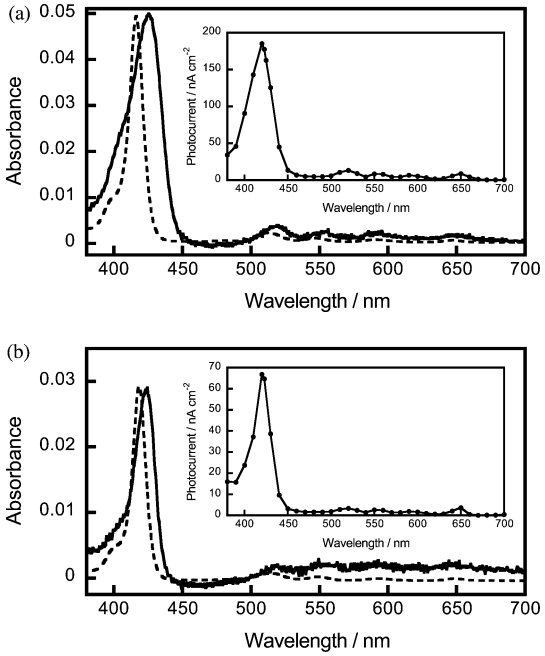

Figure 2. UV−visible absorption spectra of (a) TPP/ITO (solid line) and TPP-ref in THF (dotted line) and (b) TBPP/ITO (solid line) and TBPP-ref in THF (dotted line). The spectra are normalized at the Soret band for comparison. Action spectra of ITO/TPP/TEA/Pt (0.83 mW cm^{-2}) and ITO/TBPP/TEA/Pt (0.83 mW cm^{-2}) systems are shown as an inset. Applied potential: +0.40 V vs Ag/AgCl (sat. KCl). Nitrogen-saturated 0.1 M Na_2SO_4 aqueous solution containing 50 mM TEA.

voltammetry, atomic force microscopy (AFM), fluorescence lifetime and anisotropy measurements, and photoelectrochemical measurements. The ITO electrode was chosen because it suppresses the EN quenching of the porphyrin excited singlet state by the ITO surface.[19] Tetraphenylporphyrin (TPP) and tetraphenylpoprhyrin with bulky *tert*-butyl groups at the meta positions of the *meso*-phenyl groups (TBPP) are covalently linked to the ITO surface to give TPP/ITO and TBPP/ITO,[19] respectively. Thus, TPP/ITO and TBPP/ITO provide valuable information on the substituent effects of porphyrins on the structures and photoelectrochemical properties of the SAMs.

Results and Discussion

Preparation. The general strategy employed in preparing the SAMs is summarized in Scheme 1. Porphyrin SAMs on ITO electrodes (TPP/ITO and TBPP/ITO) were obtained by following the same procedures described previously.[19] First, activated freebase porphyrin **2** was obtained from porphyrin carboxylic acid **1**[16c,20] and pentafluorophenol.[21] Then, ITO electrodes were treated with (3-aminopropyl)trimethoxysilane by refluxing for 20 h in toluene. The activated porphyrin **2** was coupled to the (aminopropyl)silylated ITO electrodes by refluxing for 20 h in toluene to give TPP/ITO and TBPP/ITO. Porphyrin references (TPP-ref and TBPP-ref) were also synthesized by the condensation of porphyrin carboxylic acid **1** with *n*-butylamine (Figure 1). Structures of all new compounds were confirmed by spectroscopic analysis including ^{1}H NMR and MALDI-TOF mass spectra (see Experimental Section).

Spectroscopic Studies on Porphyrin SAMs. Figure 2 shows the absorption spectra of TPP/ITO, TBPP/ITO, and porphyrin references TPP-ref and TBPP-ref in THF. The Soret bands of TPP/ITO and TBPP/ITO become broader than those of TPP-ref and TBPP-ref in THF.[22] The λ_{max} value of the Soret band of TPP/ITO (428 nm) is red-shifted by 12 nm as compared with that of TPP-ref (416 nm) in THF. Similar red-shift (8 nm) was noted for the λ_{max} value of TBPP/ITO (425 nm)[19] relative to that of TBPP-ref in THF (417 nm). It should be noted here that

SCHEME 1

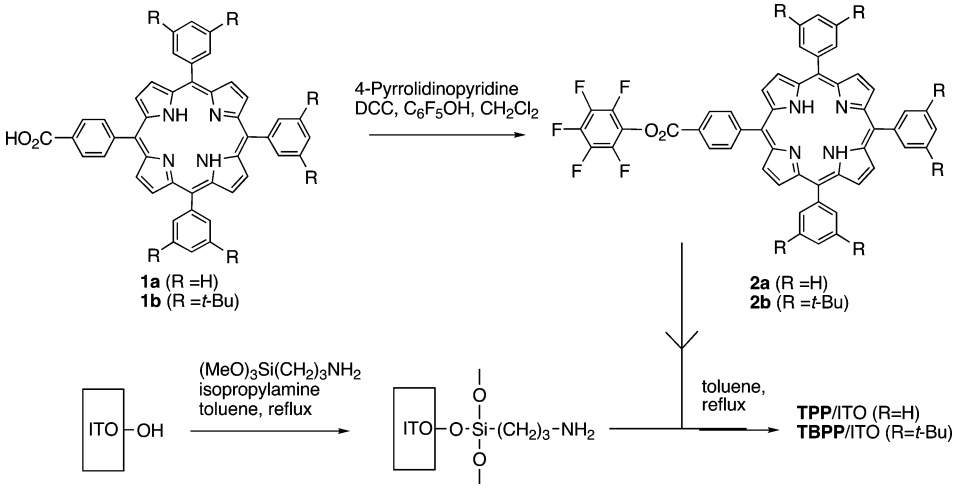

TABLE 1: Substituent Dependence of Spectral Change and Surface Coverage

	electrochemistry[a]		absorption spectroscopy			fluorescence	fluorescence
system	surface coverage/ $\times 10^{-10}$ mol cm^{-2}	molecular area/ Å^2 molecule^{-1}	absorbance[b] (λ_{max}/nm[c])	surface coverage[d]/ $\times 10^{-10}$ mol cm^{-2}	quantum yield/%[e]	lifetime/ns[f] (rel amplitude)	anisotropy lifetime/ns[f]
TPP/ITO	1.6	110	0.049 (428)	1.5	2.2 ± 0.9	1.3 (40%)	0.37
						5.9 (60%)	>10
TBPP/ITO	1.9[g]	92[g]	0.029[g] (425)[g]	0.83	3.4 ± 0.6[g]	1.9 (29%)	0.44
						8.2 (71%)	8.3
TPP-ref			(416)			10[h]	
TBPP-ref			(417)			10[h]	

[a] Measurements in CH_2Cl_2 containing 0.1 M *n*-Bu_4NPF_6 were performed with a sweep rate of 0.05 V s^{-1} (electrode area, 1.2 cm^2). [b] Absorbance at the Soret band. [c] λ_{max} at the Soret band. [d] Estimated from the UV−visible spectroscopic measurements, assuming that molar absorption coefficients of the porphyrin at the Soret band in SAMs correspond to those of the porphyrin references in THF. [e] $\phi = (i/e)/[I(1 - 10^{-A})]$, $I = (W\lambda)/(hc)$, where i is the photocurrent density, e is the elementary charge, I is number of photons per unit area and unit time, λ is the wavelength of light irradiation, A is absorbance of the adsorbed dyes at λ nm, W is light power irradiated at λ nm, c is the light velocity, and h is the Planck constant. [f] Excited at 420 nm and monitored at 650 nm. [g] From ref 19. [h] In THF.

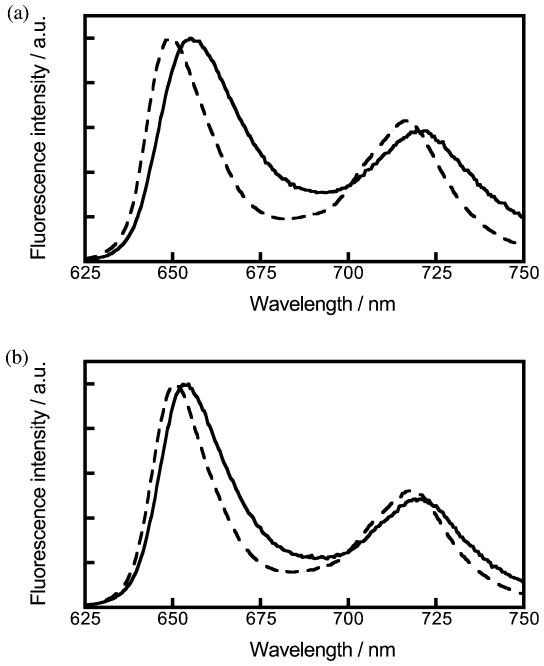

Figure 3. Fluorescence spectra of (a) TPP/ITO (solid line) and TPP-ref in THF (dotted line) and (b) TBPP/ITO (solid line) and TBPP-ref in THF (dotted line). The spectra are normalized for comparison.

the red-shift of TPP/ITO is larger than that of TBPP/ITO. These results indicate that porphyrin molecules are densely packed on the ITO surface[22,23] and the interaction between porphyrin moieties in TPP/ITO is large, as compared to TBPP/ITO, due to less steric hindrance. Assuming that the molar absorption coefficients (mol^{-1} cm^2) of porphyrin at the Soret band in TPP/ITO (4.7×10^2) and TBPP/ITO (4.3×10^2) are the same as those of TPP-ref and TBPP-ref in THF, the area of the absorption spectra provides an estimate of the surface coverage of porphyrins (Γ), after correction for surface roughness (roughness factor = 1.3, Table 1). The Γ value (mol cm^{-2}) of TPP/ITO (1.5×10^{-10}) is larger than that of TBPP/ITO (8.3×10^{-11}).[24] This difference may reflect the fact that the area of perpendicular TPP in TPP/ITO (ca. 50 Å^2 molecule^{-1})[15a] is smaller than that of perpendicular TBPP in TBPP/ITO (ca. 200 Å^2 molecule^{-1}),[16c] leading to the large Γ value of TPP/ITO relative to TBPP/ITO.

Figure 3 displays the fluorescence spectra of porphyrin SAMs and the reference compounds in THF. The spectrum of TPP/ITO becomes broader than that of TPP-ref in THF, as in the case of the absorption spectra of TPP/ITO and TPP-ref in THF. The λ_{max} values of the fluorescence spectrum of TPP/ITO (655, 720 nm) are red-shifted by 4−6 nm as compared with those of TPP-ref in THF (649, 716 nm). Similar but smaller red shifts are also seen for the λ_{max} values of TBPP/ITO (653, 721 nm) relative to those of TBPP-ref (650, 718 nm) in THF. These results are also consistent with the densely packed structures of the porphyrin SAMs where the interaction between porphyrin moieties in TPP/ITO is larger than that of TBPP/ITO, due to less steric hindrance. The energy levels of the lowest excited singlet states of TPP/ITO and TBPP/ITO were determined as +1.90 eV by the 0−0* absorption and 0*−0 fluorescence maxima in the SAMs. The energy levels of the lowest excited triplet states of TPP/ITO and TBPP/ITO were estimated as +1.49 eV by the phosphorescence maxima of TPP-ref and TBPP-ref in 2-methyl THF at 77 K.

Electrochemistry. The cyclic voltammetric measurements of TPP/ITO and TBPP/ITO in CH_2Cl_2 containing 0.2 M *n*-Bu_4NPF_6 were performed with a sweep rate of 0.05 V s^{-1} (electrode area, 1.2 cm^2) to estimate the surface coverage, as shown in Figure 4. The cyclic voltammograms of TPP/ITO and TBPP/ITO are characterized by an anodic wave showing a well-defined current maximum but smaller coupled cathodic wave on the reversed scan at 0.05 V s^{-1} due to the instability of the radical cation. The anodic current increased linearly with increasing the scan rate, implying that porphyrin is a surface-confined electroactive molecule. The E^0_{ox} values [1.05 V (TPP/ITO) and 0.98 V (TBPP/ITO) vs Ag/AgCl (sat. KCl)] were determined as the average of the anodic and cathodic peak potentials. The oxidation potentials of TBPP-ref [E^0_{ox} = 0.98 V vs Ag/AgCl (sat. KCl)] in CH_2Cl_2 and TBPP/ITO are identical, whereas the oxidation potential of TPP/ITO is shifted to the positive direction by 0.05 V relative to TPP-ref [E^0_{ox} = 1.00 V vs Ag/AgCl (sat. KCl)]. These results imply that the HOMO level of the porphyrin in TBPP/ITO is much less perturbed by the interaction with the surrounding environments than that in TPP/ITO because of less steric hindrance around the porphyrin moiety in TBPP/ITO.[25,26]

Integration of the area under the anodic waves due to the first oxidation of porphyrin provides an estimate of the surface coverage of porphyrins, Γ. The results are summarized in Table 1. Contrary to the results obtained from UV−visible absorption measurements, the Γ values of TPP/ITO (1.6×10^{-10} mol cm^{-2}) is slightly smaller than that of TBPP/ITO (1.9×10^{-10} mol cm^{-2}),[19,26] which is consistent with the ideal value where the TBPP molecules are well-packed on ITO.[16c] Although porphyrin molecules are well-packed in TPP/ITO and TBPP/ITO, there may be much free volume in TBPP/ITO than that in TPP/ITO due to the difference in steric hindrance around the porphyrin.

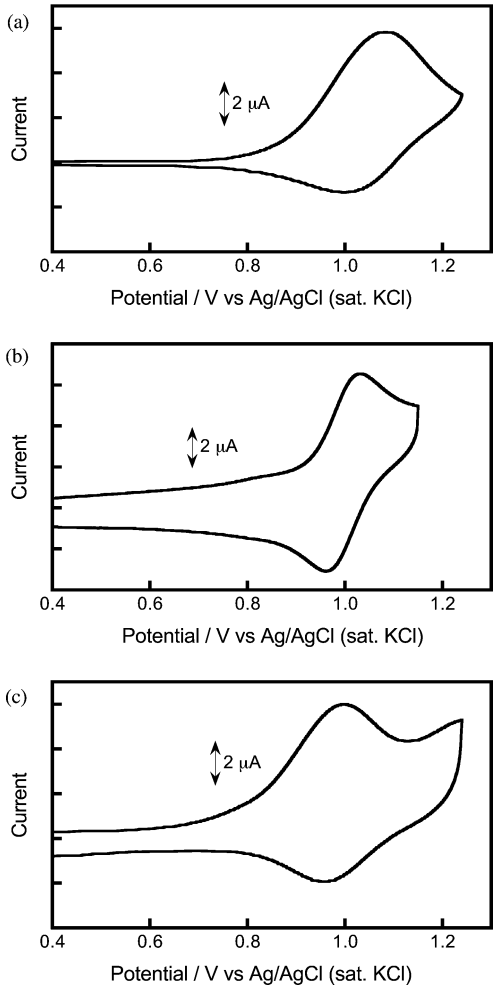

Figure 4. Cyclic voltammograms of (a) TPP/ITO, (b) TPP-ref, and (c) TBPP/ITO in CH_2Cl_2 containing 0.2 M *n*-Bu_4NPF_6 with a sweep rate of 0.05 V s^{-1}. Electrode area: 1.2 cm^2. Working electrode: the modified ITO electrode or glassy carbon electrode. Counter electrode: Pt wire. Reference electrode: Ag/Ag^+ (0.01 M $AgNO_3$, 0.1 M *n*-Bu_4NPF_6 (MeCN)). The potentials (vs Ag/Ag^+) were converted to values versus Ag/AgCl (sat. KCl) by adding 0.24 V.

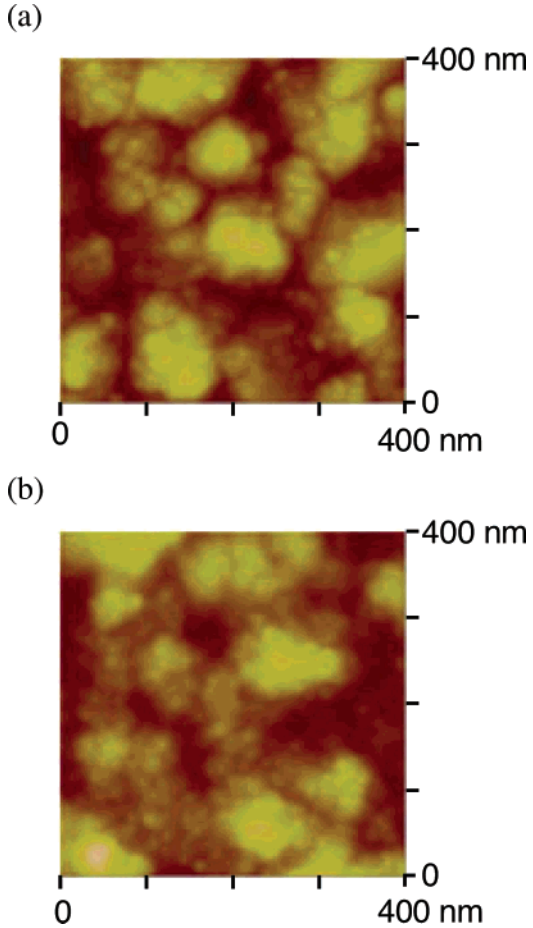

Figure 5. Tapping mode atomic force micrography of (a) TPP/ITO and (b) TBPP/ITO in air (*Z* range: 50 nm). The color scale represents the height topography, with bright and dark representing the highest and lowest features, respectively.

It is also known that the densely packed monolayer films exhibit inhibited ion transport and reduced electrochemical accessibility.[26] Thus, the coverage of TPP/ITO obtained from the cyclic voltammetry measurements is a low limit estimate, and the occupied area is an upper limit estimate due to the reduced electrochemical response.

To obtain further information on the surface structures, we performed the AFM measurements of TPP/ITO and TBPP/ITO in air with tapping mode (NanoScope IIIa, Digital Instruments). The ITO surface exhibits domain structures with a diameter of 50−100 nm and a height of ∼50 nm (Figure 5). After modification of ITO with TPP or TBPP molecules, the ITO surface shows small domain structures with a diameter of 10−30 nm, in addition to large domain structures. The small domain structures can be assigned to the porphyrin aggregates, whereas the large domain structures reflect the surface structure of rough ITO itself**.** There is no significant difference in the two AFM images, indicating that porphyrin molecules are well-packed similarly on the ITO surface.

Photoelectrochemical Measurements. Photoelectrochemical measurements were performed for TPP/ITO and TBPP/ITO in nitrogen-saturated 0.1 M Na_2SO_4 aqueous solution containing 50 mM triethanolamine (TEA) as an electron sacrificer using the modified ITO electrode as a working electrode, a platinum counter electrode, and an Ag/AgCl (saturated KCl) reference electrode (hereafter, denoted as ITO/TPP or TBPP/TEA/Pt system). Figure 6a displays currents produced by on-and-off illumination of ITO/TPP/TEA/Pt system by photoexcitation at 423 ± 5 nm with a power density of 0.83 mW cm^{-2}. The SAM showed anodic photoelectronic response when switching the light on and off, which is similar to that of the ITO/TBPP/TEA/Pt system.[19] There is a good linear relationship between the photocurrent and the light intensity at each wavelength (from 0.20 to 1.0 mW cm^{-2}). The agreement of the action spectrum with the absorption spectrum of TPP/ITO in 380−500 nm (Figure 2a) demonstrates clearly that the porphyrins are the photoactive species responsible for the photocurrent generation. In the three electrode systems, an increase in the net anodic photocurrent with an increase of the positive bias (from −200 to +500 mV) to the ITO electrode (Figure 6b), demonstrates that the electron flows from the electrolyte solution to the ITO electrode through the SAM under illumination. The dark current is much lower than the net photocurrent within the range of the applied potential to the ITO electrode.

Based on the energetics of the photoactive and radical ion species involved in ITO/TPP or TBPP/TEA/Pt system, the mechanism of photocurrent generation is shown in Scheme 2, as reported previously for ITO/TBPP/TEA/Pt system.[19] First, ET takes place from TEA [+0.61 V vs Ag/AgCl (sat. KCl)][19] to the porphyrin singlet excited state [$^1TPP^*$, +0.66 V vs Ag/AgCl (sat. KCl); $^1TBPP^*$, +0.62 V vs Ag/AgCl (sat. KCl)[19]]

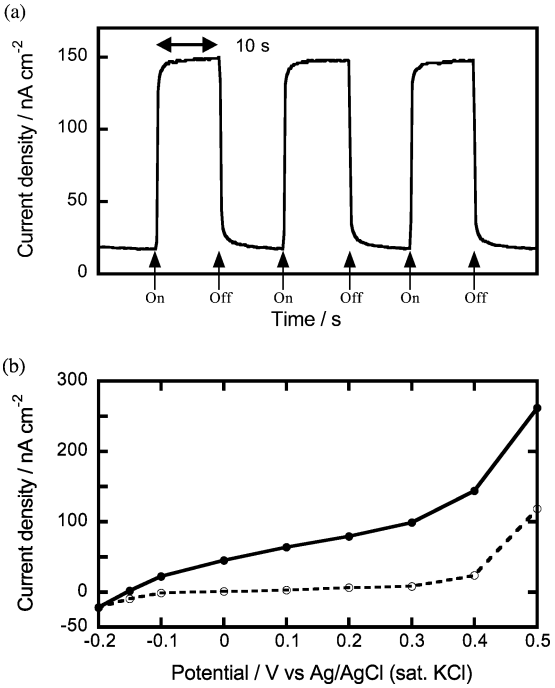

Figure 6. (a) Photoelectrochemical response of the ITO/TPP/TEA/Pt system. Applied potential: +0.40 V vs Ag/AgCl (sat. KCl). (b) Photocurrent vs applied potential curves for ITO/TPP/TEA/Pt system (solid line with closed circles). The dark currents are shown as a dotted line with open circles. $\lambda = 423 \pm 5$ nm (0.83 mW cm^{-2}). Nitrogen-saturated 0.1 M Na_2SO_4 aqueous solution containing 50 mM TEA.

SCHEME 2

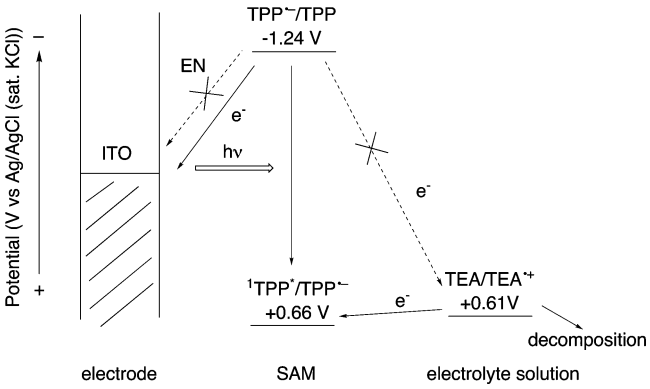

rather than the porphyrin excited triplet state [^{3}TPP*, +0.25 V vs Ag/AgCl (sat. KCl); ^{3}TBPP*, +0.21 vs Ag/AgCl (sat. KCl)], yielding the porphyrin radical anion (TPP$^{\bullet-}$ or TBPP$^{\bullet-}$) and TEA radical cation (TEA$^{\bullet+}$). TEA$^{\bullet+}$ thus formed is known to undergo irreversible decomposition via hydrogen abstracting rearrangement from another TEA,[27] which suppresses charge recombination from TPP$^{\bullet-}$ or TBPP$^{\bullet-}$ to TEA$^{\bullet+}$. The resultant porphyrin radical anion [TPP$^{\bullet-}$, −1.24 V vs Ag/AgCl (sat. KCl); TBPP$^{\bullet-}$, −1.28 V vs Ag/AgCl (sat. KCl)[19]] gives an electron to the ITO electrode, resulting in the anodic photocurrent generation. In such a case, the rate-determining step for the photocurrent generation may be the photoinduced electron transfer from TEA to $^1H_2P^*$, when the quantum yield for photocurrent generation is significantly dependent on the excited-state lifetime. Because the bulky *tert*-butyl groups are introduced at the meta-positions of the *meso*-phenyl groups on the porphyrin ring in TBPP/ITO, self-quenching due to porphyrin aggregation would be significantly reduced. In fact, fluorescence lifetime of 5,10,15,20-tetra-*p*-tolylporphyrin (TTP) in LB films (<150 ps) decreases dramatically relative to 5,10,15,20-tetrakis(3,5-di-*tert*-butylphenyl)porphyrin in LB films (1−9 ns) due to the severe self-quenching of TTP.[28] Therefore, one can expect significant enhancement of photocurrent generation efficiency in ITO/TBPP/TEA/Pt system relative to ITO/TPP/TEA/Pt system.

The internal quantum yields of photocurrent generation were compared between the ITO/TPP/TEA/Pt and ITO/TBPP/TEA/Pt systems at an applied potential of +0.40 V vs Ag/AgCl (sat. KCl) where dark current is negligible. The quantum yields (ϕ) based on the number of photons absorbed by TPP on TPP/ITO and TBPP on TBPP/ITO were calculated using the input power (P_{in}), the photocurrent density (i), and the absorbance (A) on the electrodes (ITO/TPP/TEA/Pt system: $P_{in} = 0.83$ mW cm^{-2} ($\lambda_{ex} = 423 \pm 5$ nm), $i = 140$ nA cm^{-2}, $A = 0.049$; ITO/TBPP/TEA/Pt system: $P_{in} = 0.83$ mW cm^{-2} ($\lambda_{ex} = 423 \pm 5$ nm), $i = 120$ nA cm^{-2}, $A = 0.029$). Surprisingly, the quantum yield of the ITO/TPP/TEA/Pt system ($2.2 \pm 0.9\%$) is virtually the same as that of the ITO/TBPP/TEA/Pt system ($3.4 \pm 0.6\%$) (Table 1), although there is a large difference in the interaction between porphyrins due to the absence or the presence of bulky *tert*-butyl groups.

Fluorescence Lifetime Measurements. No significant difference in the quantum yields of photocurrent generation may be explained by the photophysical properties of TPP/ITO and TBPP/ITO systems. Thus, we performed time-correlated single-photon counting fluorescence measurements on TPP/ITO and TBPP/ITO as well as TPP-ref and TBPP-ref in solutions with photoexcitation at 420 nm. In each case the fluorescence decay of the porphyrin excited singlet state ($^1P^*$) was monitored at 650 nm (Figure 7). The decay curve could be well fitted as double exponentials except for the cases of TPP-ref and TBPP-ref, and the fluorescence lifetimes (τ) are summarized in Table 1. The double exponential fluorescence decay in TPP/ITO and TBPP/ITO suggests that there are at least two types of porphyrin monolayer structures, which may result from different bonding sites on the rough ITO surface.[16d,e] In either case, the fluorescence lifetimes of TPP/ITO and TBPP/ITO are moderately reduced relative to TPP-ref ($\tau = 10$ ns) and TBPP-ref ($\tau = 10$ ns) in THF. The τ values of TPP/ITO [$\tau = 1.3$ ns (40%), 5.9 ns (60%)] are largely similar to those of TBPP/ITO [$\tau = 1.9$ ns (29%), 8.2 ns (71%)]. The weighted average lifetimes of TPP/ITO (4.1 ns) and TBPP/ITO (6.4 ns) are also largely similar. These results are consistent with the results on the quantum yields of photocurrent generation. It should be emphasized here that severe self-quenching of the porphyrin excited singlet state is significantly suppressed in TPP/ITO despite strong interaction with porphyrin in TPP/ITO relative to TBPP/ITO.

We have also carried out the picosecond fluorescence anisotropy decay measurements for TPP/ITO and TBPP/ITO. Rapid anisotropy decay is expected during the energy migration processes owing to rather random orientation of porphyrin moieties in the two-dimensional SAMs. The anisotropic decay profile of TPP/ITO probed at 650 nm exhibited two decay time constants of $\tau = 370$ ps and $\tau > 10$ ns (Table 1, Supporting Information Figure S1). Similar behavior was observed for the anisotropic decay profile of TBPP/ITO which revealed two decay components with $\tau = 440$ ps and $\tau = 8.3$ ns. The double exponential fluorescence anisotropy decay suggests that there are at least two types of porphyrin monolayer structures. This may be ascribed to different bonding sites on the ITO surface. Alternatively, the long-lived, minor components may be attributed to impurity, whereas the short-lived, major components may be due to the fast energy migration between the porphyrins. In either case, the observation demonstrates the occurrence of

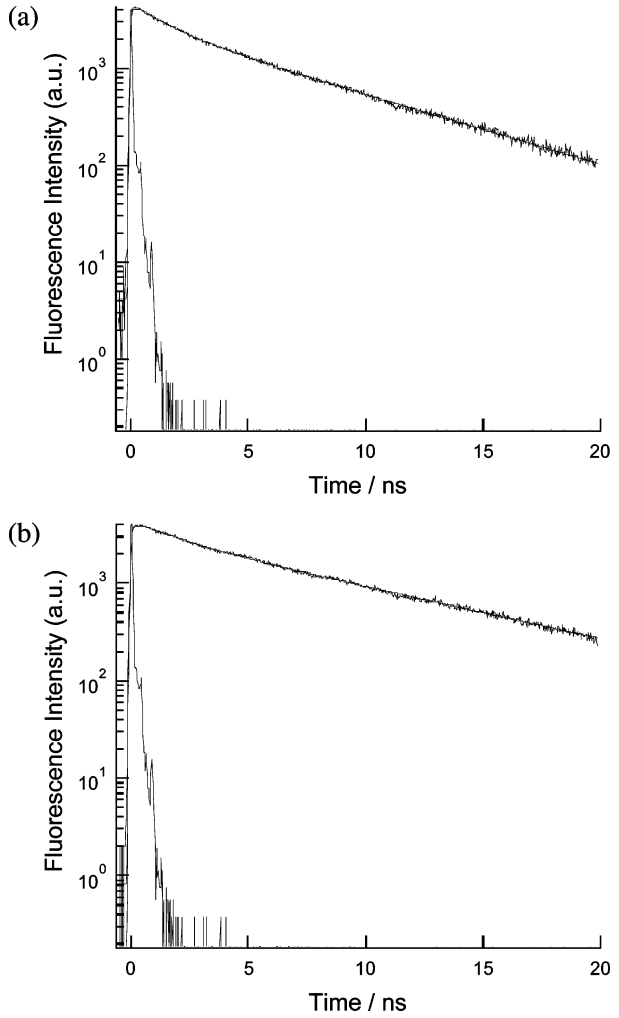

Figure 7. Fluorescence decay curves of (a) TPP/ITO and (b) TBPP/ITO observed at 650 nm by using the single-photon counting method. The excitation wavelength is 420 nm.

fast energy migration between porphyrin moieties in the SAMs. Thus, these results clearly demonstrate that the two-dimensional, densely packed structures of the porphyrins in the SAM is responsible for the long-lived porphyrin excited singlet state which is similar to the antenna function of PS1 in cyanobacteria.[5]

In conclusion, we have successfully constructed a two-dimensional, densely packed array of porphyrins on the ITO electrode where the porphyrin excited singlet state remains virtually intact irrespective of the difference in the steric hindrance around the porphyrin moieties. This conclusion is important for further development of porphyrin SAMs exhibiting antenna function, because we can densely pack porphyrin molecules on a two-dimensional electrode surface where fast energy migration takes place between the porphyrins without losing the excitation energy.

Experimental Section

General Information. Melting points were recorded on a Yanagimoto micromelting point apparatus and are not corrected. ^{1}H NMR spectra were measured on a JEOL EX-400 spectrometer. Matrix assisted laser desorption/ionization (MALDI) mass spectra (MS) were measured on Shimadzu KOMPACT MALDI II. UV−visible spectra were obtained on a Perkin-Elmer Lambda 900UV/vis/NIR spectrometer. Steady-state fluorescence spectra were acquired on a SPEX FluoroMax-3 spectrometer. Emission spectra at 77 K were obtained on a SPEX FluoroMax-II. AFM measurements were performed in air with tapping mode using NanoScope IIIa (Veeco metrology group/Digital Instruments). All solvents and chemicals were of reagent grade quality, purchased commercially, and used without further purification unless otherwise noted. Tetrabutylammonium hexafluorophosphate used as a supporting electrolyte for the electrochemical measurements was obtained from Fluka and recrystallized from methanol. Toluene and methylene chloride were dried by refluxing and distilled from CaH_2 under an argon atmosphere just before use. Thin-layer chromatography and flash column chromatography were performed with Alt. 5554 DC-Alufolien Kieselgel 60 F_{254} (Merck) and Silica gel 60N (Kanoto Chemicals), respectively. ITO electrodes (190−200 nm ITO on transparent glass slides) were commercially available from Evers, Inc. (Japan). The roughness factor (R = 1.3) was estimated by AFM measurement with tapping mode.

Synthesis of 2a. Porphyrin **1a** (0.0571 g, 0.0850 mmol) was dissolved in 20 mL of CH_2Cl_2, and 4-pyrrolidinopyridine (0.135 g, 0.911 mmol) and pentafluorophenol (0.198 g, 1.06 mmol) were added. The solution was cooled to 0 °C, and DCC (0.185 g, 0.897 mmol) was added under N_2 atmosphere. After the addition, the temperature was raised to room temperature slowly and the solution was stirred for 20 h. After the solvent was removed, the residue was purified on silica gel column chromatography (dichloromethane) and the desired porphyrin **2a** was obtained as a reddish purple solid (0.0268 g, 0.0325 mmol, 38%): mp >300 °C; ^{1}H NMR (400 MHz, $CDCl_3$) δ −2.77 (2H, s), 7.75 (9H, m), 8.21 (6H, dd, J = 2.0, 1.6 Hz), 8.40 (2H, d, J = 8.1 Hz), 8.58 (2H, d, J = 8.1 Hz), 8.80 (2H, d, J = 4.8 Hz), 8.87 (6H, m); MS(MALDI-TOF) m/z 825 ($M + H^+$).

Synthesis of TPP-ref. To a solution of **1a** (0.0379 g, 0.0564 mmol) and *n*-butylamine (0.0042 g, 0.050 mmol) in 20.0 mL of chloroform was added triethylamine (0.00508 g, 0.0503 mmol) and 1-ethyl-3-[3-(dimethylamino)propyl]carbodiimide (0.0101 g, 0.0503 mmol), and then the mixture was stirred for 18 h at room temperature under a nitrogen atmosphere. The mixture was washed with 1 M hydrochloric acid, 5% sodium bicarbonate aqueous solution, and brine successively and dried over anhydrous sodium sulfate. Flash column chromatography (chloroform:methanol = 9:1) afforded TPP-ref as a reddish purple solid (0.0175 g, 0.0245 mmol, 43.0% yield): mp >300 °C; ^{1}H NMR (400 MHz, $CDCl_3$) δ −2.79 (2H, s), 1.06 (3H, t, J = 7.2 Hz), 1.25 (2H, m), 1.77 (2H, m), 3.65 (2H, q, J = 6.4 Hz), 6.42 (1H, t, J = 6.0 Hz), 7.77 (9H, m), 8.15 (2H, d, J = 8.4 Hz), 8.21 (6H, dd, J = 2.0, 1.6 Hz), 8.29 (2H, d, J = 8.0 Hz), 8.79 (2H, d, J = 4.8 Hz), 8.85 (6H, m); FTIR (KBr) 3058, 1640, 1597, 1401, 727, 698 cm^{-1}); MS(MALDI-TOF) m/z 714 ($M + H^+$).

Synthesis of TBPP-ref. To a solution of **1b** (0.0500 g, 0.0503 mmol) and *n*-butylamine (0.0042 g, 0.050 mmol) in 20.0 mL of chloroform, was added triethylamine (0.00508 g, 0.0503 mmol) and 1-ethyl-3-[3-(dimethylamino)propyl]carbodiimide (0.0101 g, 0.0503 mmol), and then the mixture was stirred for 18 h at room temperature. The mixture was washed with 1 M hydrochloric acid, 5% sodium bicarbonate aqueous solution, brine, and dried over anhydrous sodium sulfate. Flash column chromatography (chloroform:methanol = 9:1) afforded TBPP-ref as a reddish purple solid (0.0509 g, 0.0245 mmol, 48.7% yield): mp >300 °C; ^{1}H NMR (400 MHz, $CDCl_3$), δ −2.70 (2H, s), 1.06 (3H, t, J = 7.2 Hz), 1.52 (56H, m), 1.77 (2H, m), 3.64 (2H, q, J = 6.4 Hz), 6.42 (1H, t, J = 6.0 Hz), 7.79 (3H, m), 8.07 (6H, m), 8.14 (2H, d, J = 8.0 Hz), 8.30 (2H, d, J =

8.0 Hz), 8.78 (2H, d, $J = 4.8$ Hz), 8.90 (6H, m); FTIR (KBr) 3032, 1669, 1593, 1395, 1395, 1364, 710 cm^{-1}); MS(MALDI-TOF) m/z 1051 ($M + H^+$).

Preparation of Porphyrin-Modified ITO. ITO plates were washed with MilliQ-acetone (1:1), 2-propanol, and CH_2Cl_2 for 5 min, respectively, with a sonicator, and dried under N_2 gas flow for 30 min. The ITO was soaked into the toluene solution of [3-(aminopropyl)trimethoxysilyl]amine (10% v/v) and isopropylamine (2% v/v), and N_2 gas was bubbled for 30 min. Then the solution was heated at reflux for 3 h under N_2 atmosphere. Before the solution was cooled, the ITO electrodes were rinsed with toluene and toluene/acetone (1:1) for 10 s, respectively, with a sonicator, and dried under N_2 gas flow. The rinsed ITO electrodes were soaked into the toluene solution of porphyrin **2** (5×10^{-5} M) and N_2 was bubbled for 30 min. Then the solution was heated at reflux for 3 h under N_2 atmosphere. After cooling, the modified ITO was washed twice with CH_2Cl_2 and ethanol for 10 s, respectively, with a sonicator and dried under N_2 gas flow for 30 min.

Electrochemical Measurements. All electrochemical studies were performed on a CH Instruments model 660A electrochemical workstation using a standard three-electrode cell with a modified ITO working electrode (1.2 cm^2), a platinum wire counter electrode, and an Ag/Ag^+ [0.01 M $AgNO_3$, 0.1 M n-Bu_4NPF_6 (MeCN)] reference electrode. The cyclic voltammograms of the porphyrin references and ferrocene were obtained with a glassy carbon working electrode. The potentials were calibrated with ferrocenium/ferrocene [$E_{mid} = +0.20$ V vs Ag/Ag^+; $E_{mid} = +0.44$ V vs Ag/AgCl (sat. KCl)[29]]. The adsorbed amount of porphyrin in TPP/ITO was determined from the charge of the first anodic peak of the porphyrin.

Photoelectrochemical Measurements. Photoelectrochemical measurements were performed in a one-compartment Pyrex UV cell (5 mL) under a nitrogen atmosphere.[16c] The cell was illuminated with monochromatic excitation light through a monochromator (Ritsu MC-10N) by a 500 W Xe lamp (Ritsu UXL-500D-0) on the SAM of 0.48 cm^2. The light intensity was modulated with neutral density filters (HOYA). Unless otherwise stated, nitrogen-saturated 0.1 M Na_2SO_4 and 50 mM triethanolamine (TEA) aqueous electrolyte solution was used. The photocurrent was measured in a three-electrode arrangement, a modified ITO working electrode, a platinum wire counter electrode (the distance between the electrodes is 0.3 mm), and an Ag/AgCl (saturated KCl) reference. The light intensity was monitored by an optical power meter (Anritsu ML9002A) and corrected.

Quantum yields were calculated on the basis of the number of photons absorbed by the chromophore on the ITO electrodes at 423 nm for TPP/ITO and TBPP/ITO using the input power, the photocurrent density, and the absorbance determined from the absorption spectrum on the ITO electrode.

Time-Resolved Fluorescence Lifetime and Anisotropy Measurements. A picosecond time-correlated single photon counting (TCSPC) system was employed for time-resolved fluorescence and fluorescence anisotropy decay measurements.[30,31] The system consisted of a self-mode-locked and cavity-dumped femtosecond Ti:sappahire laser pumped by a cw Nd:YAG laser (Spectra-Physics, Millennia). The full width at half-maximum of the instrument response function was 53 ps. The fluorescence decays were measured with magic angle emission polarization. Time-resolved fluorescence anisotropy decays were obtained by changing the detection polarization on the fluorescence path parallel or perpendicular to the polarization of the excitation light. Then the anisotropy decays were calculated as follows:

$$r(t) = \frac{I_{VV}(t) - GI_{VH}(t)}{I_{VV}(t) + 2GI_{VH}(t)}$$

where $I_{VV}(t)$ (or $I_{VH}(t)$) is the fluorescence decay when the excitation light is vertically polarized and only the vertically (or horizontally) polarized portion of fluorescence is detected, denoting that the subscripts stand for excitation and detection polarization, respectively. The factor G is defined by $I_{VV}(t)/I_{VH}(t)$, which is equal to the ratio of the sensitivities of the detection system for vertically and horizontally polarized light. The G factor of our detection system was 1.08. The fittings for both isotropic and anisotropic decays were performed by a least-squares deconvolution fitting process.[32] The vertical and the horizontal components of fluorescence emission were simultaneously fitted to extract the anisotropy decay functions using the LIFETIME program with an iterative nonlinear least-squares deconvolution procedure developed at the University of Pennsylvania.[33] Fluorescence decays of TPP-ref and TBPP-ref in THF were measured by using a femtosecond pulse laser excitation and a single-photon counting system for fluorescence decay measurements.[34] The laser system was a mode-locked Ti:Sa laser (Coherent, Mira 900) pumped by an argon ion laser (Coherent, Innova 300). The repetition rate of a laser pulse was 2.9 MHz with a pulse picker (Coherent, model 9200). The third harmonic generated by an ultrafast harmonic system (Inrad, model 5-050) was used as an excitation source. The excitation wavelength was set at 420 nm and temporal profiles of fluorescence decay and rise were recorded by using microchannel plate photomultiplier (Hamamatsu R3809U). The full width at half-maximum (fwhm) of the instrument response function was 36 ps, where the time interval of the multichannel analyzer (CANBERRA, model 3501) was 2.6 ps in the channel number. Criteria for the best fit were the values of χ^2 and the Dubrin-Watson parameters, obtained by nonlinear regression.

Acknowledgment. This work was supported by the Development of Innovative Technology (No. 12310) from the Ministry of Education, Culture, Sports, Science, and Technology (MEXT), Japan. H. Imahori is also thankful for a Grant-in-Aid from MEXT, Japan (21st Century COE on Kyoto University Alliance for Chemistry), for financial support. The work at Yonsei University was supported by the National Creative Research Initiative Program of the Ministry of Science and Technology of Korea.

Supporting Information Available: Fluorescence anisotropy decay profiles of TPP/ITO and TBPP/ITO. This material is available free of charge via the Internet at http://pubs.acs.org/.

References and Notes

(1) (a) *A New Developments in Construction and Functions of Organic Thin Films*; Kajiyama, T., Aizawa, M., Eds.; Elsevier: Amsterdam, 1996. (b) *A Molecular Electronics*; Jortner, J., Ratner, M., Eds.; Blackwell: Oxford, U.K., 1997. (c) *Electron Transfer in Chemistry*; Balzani, V., Ed.; Wiley-VCH: Weinheim, 2001.

(2) (a) *Anoxygenic Photosynthetic Bacteria*; Blankenship, R. E., Madigan, M. T., Bauer, C. E., Eds.; Kluwer Academic Publishers: Dordrecht, The Netherlands, 1995. (b) *The Photosynthetic Reaction Center*; Deisenhofer, J., Norris, J. R., Eds.; Academic Press: San Diego, 1993.

(3) McDermott, G.; Prince, S. M.; Freer, A. A.; Hawthornthwaite-Lawless, A. M.; Papiz, M. Z.; Cogdell, R. J.; Isaacs, N. W. *Nature* **1995**, *374*, 517.

(4) Olson, J. M. *Photochem. Photobiol.* **1998**, *67*, 61.

(5) (a) Zouni, A.; Witt, H.-T.; Kern, J.; Fromme, P.; Kraub, N.; Saenger, W.; Orth, P. *Nature* **2001**, *409*, 739. (b) Jordan, P.; Fromme, P.; Witt, H.-T.; Klukas, O.; Saenger, W.; Krauss, N. *Nature* **2001**, *411*, 909.

(6) Sener, M. K.; Lu, D.; Ritz, T.; Park, S.; Fromme, P.; Schulten, K. *J. Phys. Chem. B* **2002**, *106*, 7948.

(7) (a) Ulman, A. *An Introduction to Ultrathin Organic Films*; Academic Press: San Diego, 1991. (b) Ulman, A. *Chem. Rev.* **1996**, *96*, 1533.

(8) (a) Vincente, M. G. H.; Jaquinod, L.; Smith, K. M. *Chem. Commun.* **1999**, 1771. (b) Anderson, H. L. *Chem. Commun.* **1999**, 2323. (c) Gust, D.; Moore, T. A. In *The Porphyrin Handbook*; Kadish, K. M., Smith, K., Guilard, R., Eds.; Academic Press: San Diego, CA, 2000; Vol. 8, pp 153−190. (d) Aratani, N.; Osuka, A.; Cho, H. S.; Kim, D. *J. Photochem. Photobiol. C* **2002**, *3*, 25. (e) Wasielewski, M. R. *Chem. Rev.* **1992**, *92*, 435.

(9) (a) Lin, V. S.-Y.; DiMagno, S. G.; Therien, M. J. *Science* **1994**, *264*, 1105. (b) Yeow, E. K. L.; Ghiggino, K. P.; Reek, J. N. H.; Crossley, M. J.; Bosman, A. W.; Schenning, A. P. H. J.; Meijer, E. W. *J. Phys. Chem. B* **2000**, *104*, 2596. (c) Aratani, N.; Cho, H. S.; Ahn, T. K.; Cho, S.; Kim, D.; Sumi, H.; Osuka, A. *J. Am. Chem. Soc.* **2003**, *125*, 9668. (d) Choi, M.-S.; Aida, T.; Yamazaki, T.; Yamazaki, I. *Chem. Eur. J.* **2002**, *8*, 2667. (e) Takahashi, R.; Kobuke, Y. *J. Am. Chem. Soc.* **2003**, *125*, 2372.

(10) Kuhn, H.; Mobius, D.; Bucher, H. In *Spectroscopy of Monolayer Assemblies*; Weissberger, A., Rossiter, B. W., Eds.; Techniques of Chemistry, Vol.1; Wiley: New York, 1972.

(11) (a) Yamazaki, I.; Tamai, N.; Yamazaki, T.; Murakami, A.; Mimuro, M.; Fujita, Y. *J. Phys. Chem.* **1988**, *92*, 5035. (b) Yamazaki, I.; Tamai, N.; Yamazaki, T. *J. Phys. Chem.* **1990**, *94*, 516. (c) Fujihira, M. *Mol. Cryst. Liq. Cryst.* **1990**, *183*, 59.

(12) (a) Mallouk, T. E.; Harrison, D. J. In *Interfacial Design and Chemical Sensing*; Mallouk, T. E., Harrison, D. J., Eds.; ACS Symposium Series 561; American Chemical Society: Washington, DC, 1994. (b) Cao, G.; Hong, H.-G.; Mallouk, T. E. *Acc. Chem. Res.* **1992**, *25*, 420. (c) Kaschak, D. M.; Johnson, S. A.; Waraksa, C. C.; Pogue, J.; Mallouk, T. E. *Coord. Chem. Rev.* **1999**, *185*−*186*, 403.

(13) (a) Tkachenko, N. V.; Tauber, A. Y.; Hynninen, P. H.; Sharonov, A. Y.; Lemmetyinen, H. *J. Phys. Chem. A* **1999**, *103*, 3657. (b) Pevenage, D.; Van der Auwear, M.; De Schryver, F. C. *Langmuir* **1999**, *15*, 4641. (c) Tkachenko, N. V.; Vuorimaa, E.; Kesti, T.; Alekseev, A. S.; Tauber, A. Y.; Hynninen, P. H.; Lemmetyinen, H. *J. Phys. Chem. B* **2000**, *104*, 6371.

(14) (a) Byrd, H.; Suponeva, E. P.; Bocarsly, A. B.; Thompson, M. E. *Nature* **1996**, *380*, 610. (b) Lahav, M.; Gabriel, T.; Shipway, A. N.; Willner, I. *J. Am. Chem. Soc.* **1999**, *121*, 258. (c) Lahav, M.; Heleg-Shabtai, V.; Wasserman, J.; Katz, E.; Willner, I.; Dürr, H.; Hu, Y.-Z.; Bossmann, S. H. *J. Am. Chem. Soc.* **2000**, *122*, 11480. (d) Abdelrazzaq, F. B.; Kwong, R. C.; Thompson, M. E. *J. Am. Chem. Soc.* **2002**, *124*, 4796. (e) Ikeda, A.; Hatano, T.; Shinkai, S.; Akiyama, T.; Yamada, S. *J. Am. Chem. Soc.* **2001**, *123*, 4855.

(15) (a) Uosaki, K.; Kondo, T.; Zhang, X.-Q.; Yanagida, M. *J. Am. Chem. Soc.* **1997**, *119*, 8367. (b) Kondo, T.; Yanagida, M.; Nomura, S.-i.; Ito, T.; Uosaki, K. *J. Electroanal. Chem.* **1997**, *438*, 121. (c) Koide, Y.; Terasaki, N.; Akiyama, T.; Yamada, S. *Thin Solid Film* **1999**, *350*, 223. (d) Morita, T.; Kimura, S.; Kobayashi, S.; Imanishi, Y. *J. Am. Chem. Soc.* **2000**, *122*, 2850. (e) Kondo, T.; Yanagida, M.; Zhang, X.-Q.; Uosaki, K. *Chem. Lett.* **2000**, 964. (f) Hatano, T.; Ikeda, A.; Akiyama, T.; Yamada, S.; Sano, M.; Kanekiyo, Y.; Shinkai, S. *J. Chem. Soc., Perkin Trans. 2*, **2000**, 909.

(16) (a) Akiyama, T.; Imahori, H.; Sakata, Y. *Chem. Lett.* **1994**, 1447. (b) Imahori, H.; Norieda, H.; Ozawa, S.; Ushida, K.; Yamada, H.; Azuma, T.; Tamaki, K.; Sakata, Y. *Langmuir* **1998**, *14*, 5335. (c) Imahori, H.; Norieda, H.; Nishimura, Y.; Yamazaki, I.; Higuchi, K.; Kato, N.; Motohiro, T.; Yamada, H.; Tamaki, K.; Arimura, M.; Sakata, Y. *J. Phys. Chem. B* **2000**, *104*, 1253. (d) Imahori, H.; Arimura, M.; Hanada, T.; Nishimura, Y.; Yamazaki, I.; Sakata, Y.; Fukuzumi, S. *J. Am. Chem. Soc.* **2001**, *123*, 335. (e) Imahori, H.; Kashiwagi, Y.; Endo, Y.; Hanada, T.; Nishimura, Y.; Yamazaki, I.; Araki, Y.; Ito, O.; Fukuzumi, S. *Langmuir* **2004**, *20*, 73.

(17) (a) Imahori, H.; Azuma, T.; Ozawa, S.; Yamada, H.; Ushida, K.; Ajavakom, A.; Norieda, H.; Sakata, Y. *Chem. Commun.* **1999**, 557. (b) Imahori, H.; Azuma, T.; Ajavakom, A.; Norieda, H.; Yamada, H.; Sakata, Y. *J. Phys. Chem. B* **1999**, *103*, 7233. (c) Hirayama, D.; Yamashiro, T.; Takimiya, K.; Aso, Y.; Otsubo, T.; Norieda, H.; Imahori, H.; Sakata, Y. *Chem. Lett.* **2000**, 570.

(18) (a) Akiyama, T.; Imahori, H.; Ajavakom, A.; Sakata, Y. *Chem. Lett.* **1996**, 907. (b) Imahori, H.; Ozawa, S.; Ushida, K.; Takahashi, M.; Azuma, T.; Ajavakom, A.; Akiyama, T.; Hasegawa, M.; Taniguchi, S.; Okada, T.; Sakata, Y. *Bull. Chem. Soc. Jpn.* **1999**, *72*, 485. (c) Imahori, H.; Yamada, H.; Ozawa, S.; Ushida, K.; Sakata, Y. *Chem. Commun.* **1999**, 1165. (d) Imahori, H.; Yamada, H.; Nishimura, Y.; Yamazaki, I.; Sakata, Y. *J. Phys. Chem. B* **2000**, *104*, 2099. (e) Imahori, H.; Sakata, Y. *Adv. Mater.* **1997**, *9*, 537. (f) Imahori, H.; Sakata, Y. *Eur. J. Org. Chem.* **1999**, *2445*, 5. (g) Imahori, H.; Norieda, H.; Yamada, H.; Nishimura, Y.; Yamazaki, I.; Sakata, Y.; Fukuzumi, S. *J. Am. Chem. Soc.* **2001**, *123*, 100.

(19) (a) Yamada, H.; Imahori, H.; Nishimura, Y.; Yamazaki, I.; Fukuzumi, S. *Chem. Commun.* **2000**, 1921. (b) Yamada, H.; Imahori, H.; Nishimura, Y.; Yamazaki, I.; Fukuzumi, S. *Adv. Mater.* **2002**, *14*, 892. (c) Yamada, H.; Imahori, H.; Nishimura, Y.; Yamazaki, I.; Ahn, T. K.; Kim, S. K.; Kim, D.; Fukuzumi, S. *J. Am. Chem. Soc.* **2003**, *125*, 9129.

(20) Lindsey, J. S.; Schreiman, I. C.; Hsu, H. C.; Kearney, P. C.; Marguerettaz, A. M. *J. Org. Chem.* **1987**, *52*, 827.

(21) McCallien, D. W. J.; Burn, P. L.; Anderson, H. L. *J. Chem. Soc., Perkin Trans. 1* **1997**, 2581.

(22) Partially stacked side-by-side porphyrin aggregation (J aggregation) may be responsible for the red shift and broadening of porphyrin SAMs. A similar structure was reported for porphyrin aggregates[23] and porphyrin SAMs on gold surfaces.[16c]

(23) (a) Maiti, N. C.; Ravikanth, M.; Mazumdar, S.; Periasamy, N. *J. Phys. Chem.* **1995**, *99*, 17192. (b) Akins, D.; Zhu, H.-R.; Guo, C. *J. Phys. Chem.* **1996**, *100*, 5420. (c) Maiti, N. C.; Mazumdar, S.; Periasamy, N. *J. Phys. Chem. B* **1998**, *102*, 1528.

(24) The surface coverage obtained from absorption spectra on the ITO surface is likely to be incorrect, because the molar absorption coefficient on the ITO surface is different from that in solutions due to porphyrin aggregation.

(25) The decreased dielectric constant in the densely packed, nonpolar monolayer as compared to that of bulk solution results in the positive shift of the oxidation potential of the porphyrin.

(26) Campell, D J.; Herr, B. R.; Hulteen, J. C.; Van Duyne, R. P.; Mirkin, C. A. *J. Am. Chem. Soc.* **1996**, *118*, 10211.

(27) (a) Chan, S.-F.; Chou, M.; Creutz, C.; Matsubara, T.; Sutin, N. *J. Am. Chem. Soc.* **1981**, *103*, 369. (b) Downard, A. J.; Surridge, N. A., Gould, S.; Meyer, T. J.; Deronzier, A.; Moutet, J.-C. *J. Phys. Chem.* **1990**, *94*, 6754. (c) Matsuoka, S.; Yamamoto, K.; Ogata, T.; Kusaba, M.; Nakashima, N.; Fujita, E.; Yanagida, S. *J. Am. Chem. Soc.* **1993**, *115*, 601. (d) Aoki, A.; Abe, Y.; Miyashita, T. *Langmuir* **1999**, *15*, 1463.

(28) Anikin, M.; Tkachenko, N. V.; Lemmetyinen, H. *Langmuir* **1997**, *13*, 3002.

(29) Clérac, R.; Cotton, F. A.; Jeffery, S. P.; Murillo, C. A.; Wang, X. *Inorg. Chem.* **2001**, *40*, 1265.

(30) Lewis, C.; Ware, W. R.; Doemeny, L. J.; Nemzek, T. L. *Rev. Sci. Instrum.* **1973,** *44*, 107.

(31) Hwang, I.-W.; Cho, H. S.; Jeong, D. H.; Kim, D.; Tsuda, A.; Nakamura, T.; Osuka, A. *J. Phys. Chem. B* **2003**, *107*, 9977.

(32) Wild, U. P.; Holzwarth, A. R.; Good, H. P. *Rev. Sci. Instrum.* **1977**, *48*, 1621.

(33) Kim, Y.-R.; Hahn, J.-S.; Hong, H.; Jeong, W.; Song, N. W.; Shin, H.-C.; Kim, D. *Biochim. Biophys. Acta* **1999**, *1429*, 486.

(34) (a) Boens, N.; Tamai, N.; Yamazaki, I.; Yamazaki, T. *Photochem. Photobiol.* **1990**, *52*, 911. (b) Nishimura, Y.; Yasuda, A.; Speiser, S.; Yamazaki, I. *Chem. Phys. Lett.* **2000**, *323*, 117.